A multicell karstic aquifer model with alternative flow equations

Evangelos Rozos[1] and Demetris Koutsoyiannis

Department of Water Resources, School of Civil Engineering

National Technical University, Athens, Heroon Polytechneiou 5,

GR 15780 Zographou, Greece

Abstract

A multicell groundwater model was constructed to investigate the potential improvement in the modelling of karstic aquifers by using a mixed equation suitable for both the free surface and pressure flow conditions in karstic conduits. To estimate the model parameters the shuffled complex evolution (SCE) optimisation method was used. This ensured a fast and objective model calibration. The model was applied to two real-world karstic aquifers and it became clear that in case of absence of water level measurements, the use of the mixed equation did not improved the performance. In cases where both spring discharge and water level measurements were available, the use of the mixed equation proved to be advantageous in reproducing the features of the observed time series especially of the water level.

Keywords

Karst, Non-Darcian flow, Parameter estimation, MODFLOW

[1] Corresponding author, rozos@itia.ntua.gr

1. Introduction

Water circulation in the karstic aquifers has been classified in two types. The first one called conduit flow is similar to the turbulent flow in pipe systems and occurs in caves and conduits. The second one, generally called diffuse flow or flow in matrix, occurs in small joints and fissures and follows the principles of Darcy's law in the saturation zone (Bonacci 1987).

The models that have been used so far for karstic aquifers can be roughly classified in four main subcategories: black-box models, conceptual models, physically based models and partially physical-partially conceptual models.

In black-box models the equations and variables that are used have no physical meaning and they are similar with models of other fields. An aquifer may be regarded as a system with input I(t) (infiltration) and output Q(t) (spring discharge), which are connected with a linear differential equation. The solution of this equation is the convolution integral $Q(t) = (I * u)(t)$, where u(t) is known as kernel or response function and its identification is known as deconvolution. Dreiss (1982) used this method to determine the response function of several karstic springs in southern Missouri (USA). This work led to an understanding of the response times and quantities of groundwater moving through the system. Lambrakis et al. (2000) used a non-linear analysis of a karstic spring hydrograph. They utilised tools from literature concerning chaotic systems to achieve a short-term forecast of future behaviour of the karstic spring based only on the series of samples of the spring discharges. They also used a neural network with topology 1-3-1 (input nodes –hidden layer nodes – output nodes) as a separate approach that led to good results too. Although these models often give good results, they have the disadvantage of not providing any understanding of the physical mechanisms of the aquifer.

Conceptual models are based on simple equations that describe complex systems in a simplified but satisfactory manner. Almost 100 year ago, Maillet (1905) introduced the lumped ground water models by using a linear reservoir with a hole at the bottom to study the hydrograph of a karstic spring. The rate of the outflow is $Q = c\,H$ whereas the continuity equation is $Q\,\mathrm{d}t = A\,\mathrm{d}H$. Here c is a constant, H is the water level in the reservoir and A is the reservoir area. Combining these equations and solving the differential equation it is obtained that $Q(t) = Q_0\,\mathrm{e}^{-a\,(t-t_0)}$, where Q_0 is the discharge at time t_0 and $a := c / A$. This model may be extended to include multiple exponential recessional response elements (consequent curves with different factors a) representing the draining of conduits and aquifer matrix. Nevertheless, Nutbrown and Downing (1976) indicated that multiple recession elements might not be due to regions with varying properties. Eisenlohr (1997) showed that the coefficient a does not depend only on hydraulic properties of the aquifer but also on the area and form of the whole aquifer as well as the density of the high hydraulic conductivity conduit network.

A more complex subcategory of conceptual models uses a small number of elements or cells to represent the aquifer physical mechanisms. Barrett and Charbeneau (1997) developed a model with five reservoirs to simulate the discharge of Barton springs (USA). A novel characteristic of this model is the introduction of vertical variation in aquifer transmissivity and storativity. The model uses the Darcy equation for estimating the flow between reservoirs. Halihan et al. (1998) used only one reservoir that empties through a pipe at the bottom to model a simple and a priori known karstic formation. The equation of flow through the pipe follows a nonlinear law. An extension of this model (Halihan and Wicks, 1998) implements a number of reservoirs that communicate through pipes with turbulent flow. Using this model he

proved that constricted passages could generate a very steady response that may be interpreted as Darcian. Therefore, baseflow periods in hydrographs do not necessarily indicate that the aquifer flows under Darcian conditions. Cornaton and Perrochet (2002) suggested a porosity weighted one-dimensional differential equation, which takes into account water movement in a conduit system and water exchange within matrix continuum. In general, the models of this category are ideal in modelling cases with lack of data but they cannot apply localised information for water level fluctuation.

Physical models for karstic aquifers are considered to be those that simulate both the diffuse flow in the matrix and the flow in the pipes. One subcategory uses the double continuum approach. More specifically, the conduit system is treated as Darcian, just like the matrix, but with a higher value of hydraulic conductivity (Kiraly, 1985). Another option is to represent conduit flow as pipe flow, described by the Darcy-Weisbach equation (Mohrlok, 1997). In both models it is necessary to define an exchange term that describes the movements of water between the conduit system and the matrix. Both models have the disadvantage that they require very good knowledge of the aquifer structure and they have too many parameters to calibrate.

The equivalent continuum porous media (EPM) approach is classified in the partially physical and partially conceptual single continuum models. The underlying assumption is that the fractures are sufficiently interconnected and closely spaced to justify karst being treated as continuum with an average hydraulic conductivity on a regional scale. Larocque et al. (1999) used finite-elements and a downscaling parameterisation procedure to estimate parameters of the karstic aquifer. Based on their results they suggested that at the regional scale and in a steady-state simulation, it is not required to simulate ground water flow using a complex representation, i.e.

including the dual component of flow in the matrix and the conduit network. Sahuquillo (1983) used a finite-element method to degrade the differential equation that describes the aquifer. This equation, which may be solved analytically, is a first order non homogeneous linear differential equation of the vector of piezometric heads and includes a constant term which is the vector of sources and sinks.
Svensson (2001) suggested a method to estimate the conductivities of cells that are crossed by fractures. According to his work, a fracture contributes to the conductivity of a cell by an amount, which is equal to the intersecting volume (of fracture and cell) times the conductivity of the fracture. In this way, correlation and anisotropy structures of the aquifer are preserved.

All the studies till know use the Darcy or Darcy-Weisbach or both flow equations for modelling the karstic aquifers. The Darcy equation governs the flow in the saturated matrix of the aquifer but it is questionable if it is suitable for modelling a karstic spring that usually is the outlet of the conduit system. The Darcy-Weisbach equation applies to turbulent pressure flow; however the flow in the conduit system is not always pressurized. When the water level in the aquifer is low, then the flow in some of the conduits may be conducted with free surface conditions.

Some studies reveal that there is a non-linear relation between hydraulic conductivity K and spring discharge Q on karstic aquifers. Bonacci (2000) used the water level measured at two boreholes on the aquifer of Ombla spring, in the karst area of Croatia, to estimate the hydraulic gradient. Substituting this hydraulic gradient and the spring discharge Q to the Darcy equation he estimated the effective hydraulic conductivity K (Bonacci, 2000). The plot of the measured Q-estimated K values, forms the hysteresis loop shown in Figure 1. This significant variation of K and the hysteresis loop shown in Figure 1 must result from the stage dependent internal

routing of water and suggests that the Darcy equation with constant hydraulic conductivity is not applicable in this case.

To investigate these issues a new model was constructed which uses a flow equation that is suitable for both pressure flow and free surface flow. The model was combined with the shuffled complex evolution (SCE) optimisation method to enable automatic calibration and was applied to a virtual aquifer for validation purposes as well as to two real world aquifers to investigate the above questions.

The paper is organised as follows: Section 2 introduces the model concept and the flow equation, describes the model structure and gives comparison to the well known MODFLOW model. Section 3 gives a brief introduction to the SCE optimisation method. Section 4 describes the application of the model to two real world aquifers. Section 5 ends up with conclusions.

2. Model concept

2.1. Flow equation

The water flow through karstic aquifers, according to Brown (1972) and Cavaille (1964), is organised in three zones: The zone of aeration through which rainwater or surface runoff infiltrates the surface downwards (fractures in Figure 2), the zone of underground stream flow in which water flows vertically (shafts C1-C4 in Figure 2) and the zone of horizontal movement (gallery G in Figure 2).

The discharge Q of the karstic spring in Figure 2 equals the discharge through horizontal gallery G. It may be conjectured that this gallery may function either pressurized or as an open channel. In both cases the discharge Q can be given by the Manning formula:

$$Q = \frac{1}{n} R^{2/3} E \sqrt{J} \qquad (1)$$

where n is the Manning roughness coefficient, R is the hydraulic radius of the gallery, E is the wet cross section area and J is the hydraulic gradient.

The flow through the gallery G can be studied with the help of the simplified conceptual hydraulic structure in Figure 3. The water flows through a tunnel with height D. In case of pressure flow, R and E are constants and the discharge may be given by the formula $Q= C\sqrt{J}$ where C equals $R^{2/3}\ E\ /n$. In free surface flow both R and E depend on hydraulic depth y in the tunnel. In this case, it can be assumed that the product $R^{2/3}\ E$ is roughly a power law of y, i.e. $\beta\ (y/D)^{\alpha}$, where, β is a constant that depends on a characteristic length of the cross section (the radius for circular and the width for rectangular) and α is a constant that depends mainly on the type of the cross section. A detailed numerical investigation yields that α equals 2 for circular cross section and 1 to 5/3 for rectangular cross section with width to height ratio ranging from 0 to ∞ respectively. Substituting to the Manning formula it is concluded that $Q=\beta/n\ (y/D)^{\alpha}\ \sqrt{J}$. When $y=D$ it should be $y/D=1$ and becomes obvious that $C=\beta/n$. Combining all these it is concluded that both pressure and free surface flow can be described by:

$$Q = C\ \left(\frac{y}{D}\right)^{\alpha}\ J^{0.5} \tag{2}$$

To account for non uniform free-surface flow condition in Figure 3 and assuming that the flow is from reservoir 1 to 2 ($h_1>h_2$) the approximations $y\approx\min\left[D,(h_1+h_2)/2\right]$ and $J\approx(h_1-h_2)/L$ can be used concluding in:

$$Q = C\ \left[\min\{1,\ \frac{h_1+h_2}{2D}\}\right]^{\alpha}\ \left(\frac{h_1-h_2}{L}\right)^{0.5} \tag{3}$$

This equation can be verified by numerical hydraulic calculations. The tunnel which connects the two reservoirs in Figure 3, was assumed to have rectangular cross

section (1 m x 1 m) with n equal to 0.015, zero slope and a length of 50 m. When the tunnel functioned as an open channel, the discharge was computed solving the differential equation of non uniform flow, which gives the water depth profile. When the tunnel was pressurized, the discharge was computed using equation (1). Equation (3) was then fitted to the accurate results obtained by hydraulic calculations. The parameter C (generalised conductivity) was optimised to make the discharges calculated with (3) to fit as good as possible with the discharges calculated previously. The conductivity C was found to be 27 m^3/s while α was found 1.3. It can be observed in Figure 4 that equation (3) approximated satisfactorily the discharge in all cases examined (i.e. h_2=0, h_2=0.5 m, h_2>1 mm) even though it does not take into account the fact that the minimum hydraulic depth in the open channel of Figure 3 cannot be less than the hydraulic critical depth.

It can be noticed that if the exponent of hydraulic gradient is set to 1 instead of 0.5 and if the width to height ratio is very small, so that α equals 1, then equation (3) becomes equivalent to the Darcy equation for both confined and unconfined conditions (see equations of MODFLOW in Table 1). In this case it can be easily observed that for unconfined conditions $c = K\,D$ while for confined conditions $c = K\,\Delta z$, where K is the Darcian conductivity, c is the generalised conductivity per unit width (aggregated C over width) and Δz is the assumed layer thickness (see Table 1).

Based on these considerations, a model based on the concept of multicell models (Bear, 1979; Narasimhan and Witherspoon, 1976) that uses (3) as flow equation has been developed. The main objective of this model is to reproduce the water level fluctuation and the spring hydrograph of karstic aquifers but it is developed in a generic way so it can simulate the flow in porous media aquifers too.

For this reason multiple layers are supported, although this feature is not used in the current study, and also the option of the Darcy equation instead of equation (3) is available.

2.2 Aquifer representation

By generalisation of the scheme in Figure 3, the configuration of the entire aquifer in this multicell model is represented by a network consisting of transportation elements and storage elements (reservoirs). The catchment area is divided into surface cells. To each surface cell, shown in Figure 5 as a rectangle, which however is not restrictive, corresponds one or more vertically aligned reservoirs. The area of the base of each reservoir equals the area of the corresponding surface cell multiplied by the specific yield.

In the generic case, where more than one layers are used for modelling an aquifer, the hydraulic head in reservoir (i,j,k) with i,j the areal grid indexes and k the vertical layer index, is calculated using the following formula:

$$h_{ijk} = \begin{cases} W_{ijk} + b_k & (W_{ijk} \le \Delta z) \\ (W_{ijk} - \Delta z)\,\lambda + b_k + \Delta z & (W_{ijk} \ge \Delta z) \end{cases} \quad (4)$$

where: W_{ijk} is the water level in reservoir (i,j,k), b_k is the elevation of the bottom of layer k, h_{ijk} is the hydraulic head of the water in reservoir (i,j,k), Δz is the layer thickness and λ is the rate of specific yield to confined storage coefficient. The upper equation in (4) corresponds to phreatic conditions while the lower corresponds to confined conditions, so that the thickness Δz represents also the threshold between confined and unconfined conditions.

The volume of water contained in this reservoir is $V_{ijk} = F_{ij}\, W_{ijk}$ where F_{ij} is the area of the base of reservoirs under surface cell (i,j). Thus (4) represents the relation between hydraulic head and water contained in reservoir. As shown in the Appendix,

this equation can be easily transformed into the corresponding equations used by MODFLOW (Table 1, Relation h-V).

The water movement in the network is simulated using an explicit numerical method. Assuming a small time step, the variation of water level in reservoirs within a time step can be neglected. In each time step, equation (4) is used to compute the hydraulic gradient between two reservoirs and then the flow equation is used to calculate the specific discharge that in turn is transformed into water flux. To achieve the optimum speed and stability of the arithmetic solution, the time step is tuned during simulation. To this aim, a maximum allowed water level change in reservoirs (maxdw) within a time step and a multiplier (mdt) are used. If water level change equals maxdw within a tolerance, dt remains the same, otherwise, if water level change is lower or higher, dt is multiplied or divided respectively by mdt.

The boundary conditions are implemented by choosing appropriate base and water level of reservoirs. The constant head can be modelled by choosing a reservoir with very large base. Due to the large base, the water level in reservoir remains practically constant and close to the prescribed boundary condition value. A spring is modelled again by a reservoir with very large base that can only take water from neighbouring reservoirs. Simulations of the slight changes of water level in this reservoir can be directly transformed into spring hydrograph.

The stresses are applied as changes to water level in reservoirs. The recharge is applied to the highest active reservoir by gradually increasing the water level in a stress period. Abstractions due to pumping decrease water level of pumped reservoirs.

To represent the aquifer by the network of reservoirs and transportation elements, the grid topology and the set of hydrogeologic parameters are needed. The grid topology is determined by the coordinates of the centres of reservoirs and the

corresponding surface cell areas. The hydrogeologic parameters are the specific yield S_Y (it affects the reservoir bases), the generalised conductivities per unit width c between reservoirs, the layer thickness Δz, and parameters α, D (equation (3)) and λ (equation (4)). The flow equation solver needs the initial time step, the maximum allowed water level change (maxdw) and the time step multiplier (mdt).

The proposed model was named 3dkflow after 3D karstic flow model. To make more clear the basic features of 3dkflow, a comparison to the standard groundwater model MODLFOW is useful:

- The equations that are used by both 3dkflow and MODFLOW (McDonald and Harbaugh, 1988) assuming one layer (for simplicity) are shown in Table 1.
- In MODFLOW the flow equation and the relation between h and V are substituted to the continuity equations of all cells resulting in a set of linear equations (implicit scheme). The solution of this linear equations set gives the hydraulic head at the centres of the cells. In 3dkflow the continuity equation is solved sequentially for all reservoirs individually (explicit scheme).
- Both MODFLOW and 3dkflow use internode conductivities in calculations. The input files of MODFLOW contain block centred cell parameters so that an averaging (arithmetic, harmonic or geometric) is necessary to get the internode conductivities. The input files of 3dkflow contain directly the internode conductivities. This is a better choice in case that the parameters are estimated only via the model (lack of field measurements of parameters) because it skips the unnecessary averaging during the optimisation procedure.

The integrity of 3dkflow was verified by means of comparisons with MODFLOW (version 96). A virtual rectangular phreatic aquifer with a spring outlet at one corner was represented by a 10x17 grid and it was solved with both models (the Darcy

equation is selected in 3dkflow). The simulated time series of water level at two cells (namely (6,4) and (7,14)) and spring discharge obtained by two models were compared and the coefficients of determination (also known as Nash's index) were found to be very close to 1. The slight departures from 1 are explained by the fact that the input files of MODFLOW contain cell conductivities while the input files of 3dkflow contain internode conductivities. In terms of the time needed by the two models to complete the simulation, MODFLOW appears to be 10 times faster than 3dkflow. This was expected since MODFLOW uses an implicit arithmetic solution scheme while 3dkflow uses an explicit scheme that calls for small time steps to maintain the stability and accuracy of the solution.

3. The shuffled complex evolution method

To estimate the parameters of the aquifer, 3dkflow must be combined with an efficient optimisation algorithm. In this study the shuffled complex evolution method (SCE) (Duan et al., 1992) has been adopted. This is a heuristic global optimisation scheme that combines the strength of the downhill simplex procedure of Nelder and Mead (1965) with the concepts of controlled random search (Price, 1965), competitive evolution (Holland, 1975) and complex shuffling. This method has become the most popular among hydrologists and many references about it can be found in the water resources literature (Duan et al. 1994; Gan and Biftu, 1996; Cooper et al., 1997; Kuczera, 1997; Yapo et al., 1998; Freedman et al., 1998; Thyer et al., 1999).

The algorithm begins by randomly selecting a population of feasible points that are sorted and partitioned into a number of communities (complexes). Each of the complexes is allowed to evolve in the direction of global improvement, using

competitive evolution techniques that are based on the downhill simplex method. At periodic stages in the evolution, the entire set of points is shuffled and reassigned to new complexes to enable information sharing. This process is repeated until some stopping criteria are satisfied.

The SCE algorithm was incorporated into 3dkflow to facilitate the calibration of the model. The parameters that are optimised by the SCE algorithm are the generalised conductivities, the specific yield and the parameter D (the exponent α is optimised manually, trying a set of likely values). The number of parameters depends on the dimensions of the aquifer model and on the spatial distribution of generalised conductivities. The simplest possible model consists of two reservoirs connected with one transportation element. In this case the model includes only three parameters (generalised conductivity of the transportation element, specific yield of reservoirs and D). In two- or three-dimensional models the number of parameters is greater but even in these cases the SCE algorithm proved to be satisfactory.

4. Case studies

Two of the most important karstic aquifers in Greece were modelled with 3dkflow. The first discharges at the Almiros spring located at the North coast of Eastern Crete near Agios Nikolas and the second discharges at the Lilea spring located at the foot of Parnasos mountain 130 km northwest of Athens. Equation (3) and Darcy equation were used alternatively in the two simulations and the results were compared to identify differences in performance.

The surface geological formations of the Almiros spring area are displayed in Figure 6 and the geological layering in Figure 7. The spring drains a dolomitic limestone aquifer, which lies on phyllite-quartzite series (IGME, 1977). The spring is

located at a distance of 50 meters from the sea at an elevation of +0.7 m above sea level (masl). The discharge varies between 1.5 and 3 m^3/s. The mean annual discharged volume of the spring is 64 hm^3 while 11 hm^3 of water are pumped during April to October from the aquifer for irrigation. That suggests a total outflow of 75 hm^3 per year from the aquifer. The rainfall at the mean basin elevation (600 m) is 1185 mm while IGME (1996) estimated that the annual evapotranspiration equals 575 mm. They also estimated the recharge to aquifer as 491 mm and the catchment area as 152 km^2.

The period of available measurements is from January 1977 to September 1985. The spring discharge measurements are performed with average frequency once a week (IGME, 1990). Infrequent water level measurements are performed only in two places in the area at boreholes F16 and D3 (Figure 6). The mean water level at them is 223.5 and 15.7 masl.

The estimated spatial deployment of the catchment area is shown in Figure 6 and the discretisation that was used to model the aquifer is shown in Figure 8. Three zones of conductivities along x-direction were assumed. This zonation pattern is suggested by the observed water level gradient, which is very steep at the Xeropotamos area, possibly because of an alluvium curtain (IGME, 1990). The first and third zones are assumed to have equal x-direction conductivities ($K_{x,1}$ for Darcy, $c_{x,1}$ for the equation (3)) while the x-direction conductivity in second zone ($K_{x,2}$ for Darcy, $c_{x,2}$ for the equation (3)) is expected to be much lower. Constant conductivity along y (K_y for Darcy, c_y for the equation (3)) and constant specific yield (S_Y) were used. The parameters D and α of equation (3) were constant also. The conductance Cd and the generalised conductivity to spring reservoir (C) are used to regulate the spring discharge when using Darcy equation and when using the equation (3) respectively.

One layer with 5x8 cells was proved to be a sufficient for representing the two wells, the three zones of conductivity and the steep hydraulic gradient near the spring. Denser grids were tried but they did not provide better results.

The monthly rainfall time series was filtered through a modified Thornthwaite (1948) model to calculate the infiltration to deeper aquifer that is the input to 3dkflow. The crops at Drasi, Xeropotamos, North Lakonia and South Lakonia are irrigated using groundwater. The reservoirs of the cells 22, 23, 24-14 and 34 (Figure 8) were pumped from April to October, to model the releases for the irrigation.

The objective function to be minimized is the weighted mean square error between simulated and measured time series of spring discharge. The calibration period extends from October 1977 to September 1985. The period from January 1977 to October 1977 is considered as warm up period for the model.

The estimated parameters for the equation (3) are shown in Table 3 and for the Darcy equation are shown in Table 4. The estimated conductivities of the second zone are in both equations smaller than those of first and third zone, as expected from the geological study. Also the estimated conductivities with equation (3) and with Darcy equation verify approximately the formula $c = K D$. The estimated specific yields for both equations are relatively close.

The coefficients of determination for the spring discharge (simulated and observed) and the biases in simulated water levels (differences of simulated and observed water level mean values) are shown in Table 5. The simulated spring discharge, almost identical for both equations, is shown in Figure 9. The coefficient of determination values are rather low because of the use of monthly rainfall time series and the tide effects that corrupt the measurements of spring discharge (IGME 1990,

IGME 1996). Both equations gave water levels fluctuation close to the observed range.

In the second case study, the Lilea spring discharges at an elevation of 299 meters. It is an overflow spring that drains a limestone aquifer located at the contact with alluvial deposits. The surface geological formations of the Lilea spring area are displayed in Figure 10 (IGME, 1962).

The estimated catchment area that drains through Lilea springs is about 8 km^2. However the exact geometry of the aquifer is not known. The mean annual spring yield is 9.3 hm^3 while 0.5 hm^3 is pumped during June to September for irrigation. The mean annual rainfall of the catchment is 1582 mm.

The available measurements of spring discharge and water level were performed twice a month and cover two periods, October 1980 to September 1989 (IGME 1994) and October 1993 to September 2000 (E. Dandolos, personal communication). Water level measurements are available only for the second period from the EAP5 borehole (Figure 10). Each of the two periods was used either for calibration or validation. The two calibration-validation periods extend from March 1981 to September 1989 and from March 1994 to September 2000 (October 1980 to March 1981 and October 1993 to March 1994 were the model warm up periods).

Due to the incomplete knowledge of the catchment shape and topology a parsimonious representation of the aquifer was preferred. Three reservoirs were used in modelling; the fist and the second one correspond to the distant and close to the spring aquifer areas and the last one is the spring reservoir. The model parameters were the conductivity between first and second reservoir (K_x for Darcy, c_x for the equation (3)), the conductance (Cd) for Darcy equation or the generalised conductivity (c) for equation (3) to the spring reservoir and the specific yield (S_Y).

The daily rainfall values were filtered through a modified Thornthwaite (1948) model to calculate infiltration. Then daily infiltration was upscaled to monthly infiltration for compatibility with the stress period's length of the model. The releases for irrigation were modelled with a pump from the second reservoir.

In the first calibration case (based on data of the first period of observations) the objective function to be minimized was the mean square error between simulated and observed time series of spring discharge. In the second calibration case (based on data of the second period of observations) in addition to this criterion, the weighted mean square error between simulated and observed time series of water level was also used and the two criteria were combined assuming equal weights.

Table 6 shows the estimated parameters for the equation (3) for the two periods of available data. The estimated parameters of the Darcy equation are shown in Table 7. The conductivity is rather higher than the expected value from the literature. This happens because this optimised parameter is the effective and not the real conductivity of karst matrix. The estimated specific yield in period 1994-2000 is almost twice the estimated specific yield in period 1981-1989 for both equations suggesting that the combination of water level and spring discharge measurements is critical for the estimation of a reliable value for specific yield. In other words the problem is ill-posed when either water level or spring discharge measurements are absent. The magnitude of conductivity estimated from equation (3) and that estimated from Darcy equation are compatible to each other in terms of the formula $c = K D$.

The parameters estimated in period 1981-1989 were used for validation in period 1994-2000 and vice versa concluding in two validation periods. The coefficient of determination values of the optimisations and validations for Darcy and for the equation (3) are shown in Table 8. Equation (3) achieved slightly better results for

spring discharge, and much better for water level and especially in the validation period 1994-2000 (Figure 11). The simulation of spring discharge for (3) in period 1994-2000 is shown in Figure 12. The model performance is acceptable taking into account the coarse spatial and temporal (monthly infiltrations) discretisation.

Equation (3) achieved better performance in the two validations although the parameters for the two periods are not quite close. Increasing the conductivity and decreasing the specific yield results in a more sharp response of the aquifer and vice versa. That means that the ratio c/S_Y is a quantitative index of the aquifer behaviour. The ratio c/S_Y for equation (3) and the period 1981-1989 is 0.34 m^2/s and for the period 1994-2000 is 0.32 m^2/s i.e. quite close. In the Darcy equation the ratio Cd/S_Y is 2.25 m^2/s for the period 1981-1989 and 1.4 m^2/s for the period 1994-2000. This explains the difference in performance of the two equations.

The experiment conducted by Bonacci, on the aquifer of Ombla spring, which was described in the introduction, was repeated with the Lilea spring aquifer but using simulated (by equation (3)) rather than observed data. The model parameters were those of the period 1994-2000. The simulated water level at first and second cells of Lilea model, as well as the simulated spring discharge, where used to estimate the effective hydraulic conductivity. The plot of the simulated Q-estimated K values is shown in Figure 13 and it looks similar to that in Figure 1 although the parameters of the model were constant during the simulation. This indicates that the model based on equation (3) captures the hysteresis behaviour of aquifer.

5. Conclusions

1. From this study it became clear that the Darcy equation may be not appropriate for modelling karstic aquifers, in the case where combined spring

discharge and water level measurements exist. Specifically the Darcy equation is not suitable for reproducing both discharge and water level time series and capturing the hysteresis loop between effective hydraulic conductivity and spring discharge. In this case a mixed equation that takes into account both free surface and pressurized flow in karstic conduits was proved to improve the model performance compared to the Darcy equation.

2. In the case where only spring discharge measurements are available, the use of the mixed flow equation does not improve the model performance in comparison to the Darcy equation.

Acknowledgments. The authors wish to thank Elias Dandolos, associate director of Institute of Geological and Mineral Explorations (IGME) Hydrogeology Department for the supply of Lilea spring hydrogeologic data for period from October 1993 to September 2000 and Demetris Rozos, director of IGME Technical Geology Department for the advice concerning the geology of the studied areas. Andreas Eustratiadis deserves special thanks for his help on the SCE optimisation method. The detailed review comments by Marek Nawalany and an anonymous reviewer of the initial version of this paper and the suggestions by the editor M. Sophocleous are gratefully acknowledged as they resulted in a significant improvement of this study.

References

Barrett, M.E. and Charbeneau, R.J. 1997. A parsimonious model for simulating flow in a karst aquifer. Journal of Hydrology, 196, pp. 47-65

Bear *Hydraulics of groundwater*, McGraw-Hill, New York (1979)

Bonacci, O., 1987. Karst Hydrology, Springer-Verlag, Berlin, pp. 79

Bonacci, O., 2000. Heterogeneity of hydrologic and hydrogeologic parameters in karst: example from Dinaric karst, Proceedings of the 6th International Symposium and Field Seminar, Marmaris, Turkey, 17-26 September 2000, pp 393-399.

Brown, R., H., Konoplyantsev, A.A., Ineson J., Kovalevsky V.S., A contribution to the International Hydrological Decade, Unesco Paris 1972

Cavaille, A. 1964. Observations sur l' evolution des grottes. Int. J. Speleol., vol. I, parts 1-2, p. 71-100.

Cooper, V. A, Nguyen, V. T. V., Nicell, J. A., 1997. Evaluation of global optimisation methods for conceptual rainfall-runoff model calibration, *Water Science and Technology*, 36(5), pp. 53-60.

Cornaton, F., Perrochet, P., 2002. Analytical 1D dual-porosity equivalent solutions to 3D discrete single-continuum models. Application to karstic spring hydrograph modelling, *Journal of Hydrology*, 262, pp. 165-176.

Duan, Q., Sorooshian, S., Gupta, V., 1992. Effective and efficient global optimization for conceptual rainfall-runoff models, *Water Resources Research*, 28(4), pp. 1015-1031.

Duan, Q., Sorooshian, S., Gupta, V., 1994. Optimal use of the SCE-UA global optimization method for calibrating watershed models, *Journal of Hydrology*, 158, pp. 265-284.

Dreiss, S.J., 1982. Linear kernels for karst aquifers. *Water Resources Researc*h v. 18, no. 4, pp. 865-876.

Eisenlohr, L., Király, L., Bouzelboudjen, M. and Rossier, Y., 1997. Numerical simulation as a tool for controlling the interpretation of karst spring hydrographs. *Journal of Hydrology* 193, pp. 306–315.

Freedman, V.L., Lopes, V.L. and Hernandez, M., 1998. Parameter identifiability for catchment–scale erosion modeling: a comparison of optimization algorithms. *Journal of Hydrology* 207, pp. 83–97

Gan T.Y. and G.F. Biftu , 1996. Automatic calibration of conceptual rainfall-runoff models: optimization algorithms, catchment conditions, and model structure. *Water Resources Researc*h 32 12, pp. 3513-3524

Halihan, T., Wicks, C. and Engeln, J., 1998. Physical response of a karst drainage basin to flood pulses: example of the Devil's Icebox cave system (Missouri, USA). *Journal of Hydrology* 204 1-4, pp. 24-36

Halihan, T., Wicks, C.M., 1998. Modeling of storm responses in conduit flow aquifers with reservoirs, *Journal of Hydrology*, 208, pp. 82-91.

Holland, J. H. *Adaptation in Natural and Artificial System*s, University of Michigan Press, AnnArbor (1975).

IGME, 1962. Geologic map of Greece 1:50000, sheet Amfiklia.

IGME, 1977. Geologic map of Greece 1:50000, sheet Ayios Nikolaos.

IGME, 1990. Hydrogeology investigation report of Almyros spring (Ayios Nikolaos),

IGME, 1994. Hydrogeologic investigation of Veotikos Kifissos basin.

IGME, 1996. Hydrogeology of limestone aquifers of area of Ayios Nikolaos (Crete, Greece).

Kiraly, L, 1985. FEM301, A three dimensional model for groundwater flow simulation. NAGRA Technical report, pp. 84-89, 96p.

Kuczera, G., 1997. Efficient subspace probabilistic parameter optimization for catchment models, *Water Resources Researc*h, 33(1), pp. 177-185.

Lambrakis, N., Andreou, A.S., Polydoropoulos, P., Georgopoulos, E., Bountis, T., 2000. Nonlinear analysis and forecasting of a brackish karstic spring. Water Resour. Res. v. 36, no. 4, pp. 875-884.

Larocque, M., Banton, O., Ackerer P. and Razack, M., 1999. Determining Karst Transmissivities with Inverse Modeling and an Equivalent Porous Media., Ground Water 37, no. 6, pp. 897-903.

Maillet, E., 1905. Essai d'hydraulique souterraine et fluviale: Librairie scientifique. Hermann, Paris.

McDonald Michael G. and Harbaugh Arien W. MODFLOW A Modular Three-Dimensional Finite-Difference Ground-Water Flow Model, Book 6, USGS,1988.

Mohrlok, U., Sauter, M., 1997. Modelling groundwater flow in a karst terrane using discrete and double-continuum approaches; importance of spatial and temporal distribution of recharge. In: Proc. 6th Conference on Limestone Hydrology and Fissured Media, La Chaux-de-Fonds, Switzerland, pp. 167-170.

Narasimhan, T.N. and Witherspoon, P.A., 1976. An integrated finite difference method term for analyzing fluid flow in porous media. Water Resour. Res. 12, pp. 57–64.

Nelder, J. A. and Mead R., 1965. A simplex method for function minimization, *Computer Journa*l, 7(4), pp. 308-313.

Nutbrown, D.A., Downing, R.A., 1976. Normal-mode analysis of the structure of baseflow-recession curves, *Journal of Hydrology*., 30, pp. 327-340.

Price, W.L., 1965. A controlled random search procedure for global optimisation, In: L.C.W. Dixon and G.P. Szego, Editors, Towards Global Optimization, vol. 2, North-Holland, Amsterdam (1978).

Sahuquillo, A., 1983. An eigenvalue numerical technique for solving unsteady linear groundwater models continuously in time. *Water Resources Researc*h v. 19, no. 1, pp. 87-93.

Svensson, U., 2001. A continuum representation of fracture networks. Part I: Method and basic test cases, *Journal of Hydrology*, 250, pp. 170-186.

Thyer, M., Kuczera G., Bates B. C., 1999. Probabilistic optimization for conceptual rainfall-runoff models: A comparison of the shuffled complex evolution and simulated annealing algorithms, *Water Resources Researc*h, 35(3), pp. 767-773.

Thornthwaite, C. W., 1948. An approach towards a rational classification of climate, Geographical Rev., 38, pp. 55-94.

Yapo, P. O., Gupta H. V., Sorooshian S., 1998. Multi-objective global optimization for hydrologic models, *Journal of Hydrolog*y, 204, pp. 83-97.

Table 1: Comparative presentation of equations used in MODFLOW and 3dkflow.

Model	Flow equation	Relation h – V
MODFLOW	$Q_x = K_x \Delta y \Delta z \frac{h_i - h_{i+1}}{L_x}$ if h^{m-1}>TOP	$\Delta V = S_Y (\Delta x \Delta y) \Delta h$ if h^m, h^{m-1}<TOP
		$\Delta V = S (\Delta x \Delta y) \Delta h$ if h^m, h^{m-1}>TOP
	$Q_y = K_y \Delta x \Delta z \frac{h_i - h_{i+1}}{L_y}$ if h^{m-1}>TOP	$\Delta V = (S_Y(h^m - TOP) + S(TOP - h^{m-1})) \Delta x \Delta y$ if h^m<TOP h^{m-1}>TOP
	$Q_x = K_x \Delta y \frac{h_i^2 - h_{i+1}^2}{2L_x}$ if h^{m-1}<TOP	$\Delta V = (S(h^m - TOP) + S_Y(TOP - h^{m-1})) \Delta x \Delta y$ if h^m>TOP h^{m-1}<TOP
	$Q_y = K_y \Delta x \frac{h_i^2 - h_{i+1}^2}{2L_y}$ if h^{m-1}<TOP	
3dkflow	$Q_x = c_x \Delta y \left[\min\{1, \frac{h_i + h_{i+1}}{2D}\}\right]^{\alpha} (\frac{h_i - h_{i+1}}{L_x})^{0.5}$	$h = \frac{V}{F} + b$ if $W = \frac{V}{F} < \Delta z$
	$Q_y = c_y \Delta x \left[\min\{1, \frac{h_i + h_{i+1}}{2D}\}\right]^{\alpha} (\frac{h_i - h_{i+1}}{L_y})^{0.5}$	$h = (\frac{V}{F} - \Delta z) \lambda + b + \Delta z$ if $W = \frac{V}{F} > \Delta z$

See explanation of notation in Table 2

Table 2: Notation used in Table 1.

Q_x, Q_y	discharge between reservoirs or cells (i, j) and (i, j+1) , (i+1, j)
c_x, c_y	generalised conductivities per unit width between reservoirs (i, j) and (i, j+1), (i+1, j)
K_x, K_y,	conductivities between cells (i, j) and (i, j+1), (i+1, j)
h_i, h_{i+1}, h_{j+1}	hydraulic head at reservoirs or cells (i, j), (i+1,j), (i,j+1)
L_x, L_y	distance between centres of reservoirs or cells (i, j) and (i,j+1), (i+1,j)
Δx, Δy	size of surface cell (i, j)
Δz	layer thickness
TOP	elevation of the top of the layer
b	elevation of the bottom of the layer
F	area of the base of reservoir which corresponds to surface cell (i, j)
ΔV	change of water volume in cell (i, j) from time m-1 to m
V	water volume in a reservoir (i, j) at time m
Δh	change of hydraulic head in cell or reservoir (i, j) from time m-1 to m
h^{m-1}, h^m	hydraulic head in cell or reservoir (i, j) at time m-1 and time m
h	hydraulic head in reservoir (i, j) at time m
W	Water level in reservoir (i, j) at time m
S	confined storage coefficient
S_Y	specific yield
λ	S_Y to S rate
α	exponent of flow equation
D	threshold between free surface and pressurized flow

Note: reservoirs refer to 3dkflow, cells refer to MODFLOW and surface cells refer to both.

Table 3: Estimated parameters of the Almiros aquifer model for (3) with α=1.5.

$c_{x,1}$ (m^2/s)	0.328
$c_{x,2}$ (m^2/s)	0.0017
c_y (m^2/s)	0.039
c (m^2/s)	0.399
D (m)	10.0
S_Y	0.07

Table 4: Estimated parameters of the Almiros aquifer model for Darcy.

$K_{x,1}$ (m/s)	0.04
$K_{x,2}$ (m/s)	0.00019
K_y (m/s)	0.008
Cd (m^2/s)	2.79
S_Y	0.04

Table 5: Differences of simulated and observed water level mean values and coefficients of determination for simulated spring discharge of the Almiros aquifer model.

	Bias F16 (m)	Bias D3 (m)	Coefficient of determination Spring
Equation (3)	0.47	-0.50	0.63
Darcy	0.71	-0.42	0.63

Table 6: Estimated parameters of the Lilea aquifer model for the equation (3) with α=1.4.

	1981-1989	1994-2000
c_x (m^2/s)	0.184	0.137
c (m^2/s)	0.027	0.045
D (m)	3.9	4.47
S_Y	0.08	0.14

Table 7: Estimated parameters of the Lilea aquifer model for Darcy.

	1981-1989	1994-2000
K_x (m/s)	0.017	0.017
Cd (m^2/s)	0.09	0.14
S_Y	0.04	0.10

Table 8: Coefficient of determination values for optimisation and validation of the Lilea aquifer model.

Case	Time series	Darcy	Equation (3)
Optimisation 1981-1989	Spring discharge	0.76	0.79
Validation 1981-1989	Spring discharge	0.63	0.74
Optimisation 1994-2000	Water level at EAP5	0.38	0.50
	Spring discharge	0.71	0.75
Validation 1994-2000	Water level at EAP5	-1.96	0.28
	Spring discharge	0.74	0.72

List of figures

Figure 8: 5x8 discretisation of the Almiros spring aquifer where the dark and grey rectangles represent areas with generalised conductivity $c_{x,1}$ and $c_{x,2}$ respectively, and white rectangles represent no flow areas. The irrigated areas with pumped water are marked with x. The two cells closer to the observations wells are marked with dots (left F16, right D3).

Figure 9: Observed and simulated discharge of the Almiros spring.

Figure 10: Geologic map of the Lilea spring aquifer according to IGME 1962 (Q alluvial deposits, K limestones) also indicating the location of the observation well EAP5.

Figure 11: Observed and simulated water level at the EAP5 borehole in period 1994-2000 with parameters optimised for period 1981-1989.

Figure 12: Observed and simulated spring hydrographs of the Lilea spring after optimisation in period 1994-2000.

Figure 13: Estimated effective hydraulic conductivity using data from Lilea Aquifer model.

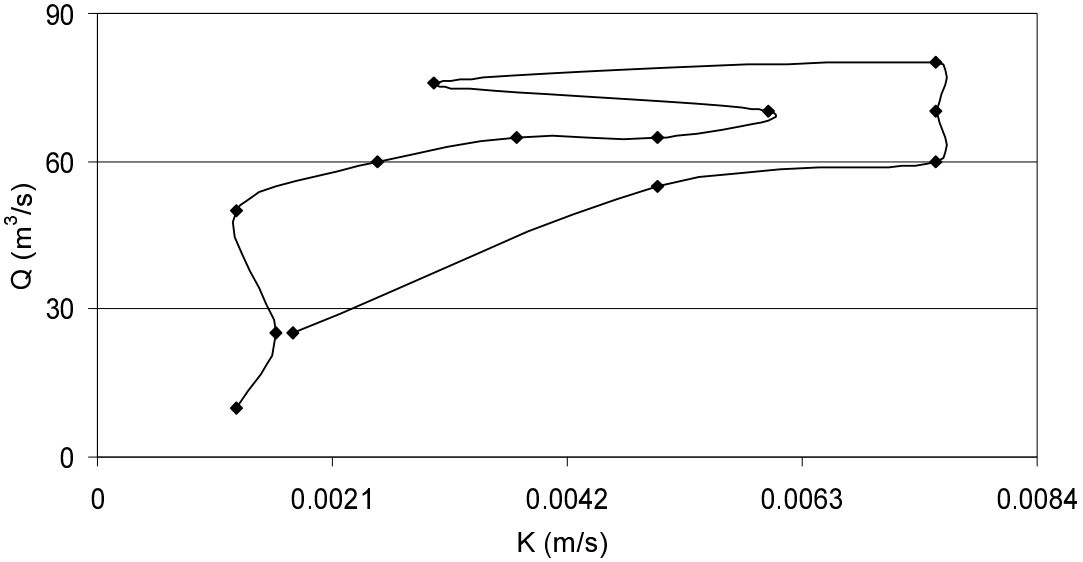

Figure 1: *Q-K* hysteresis at Ombla Spring in the karst area of Croatia (Bonacci, 2000).

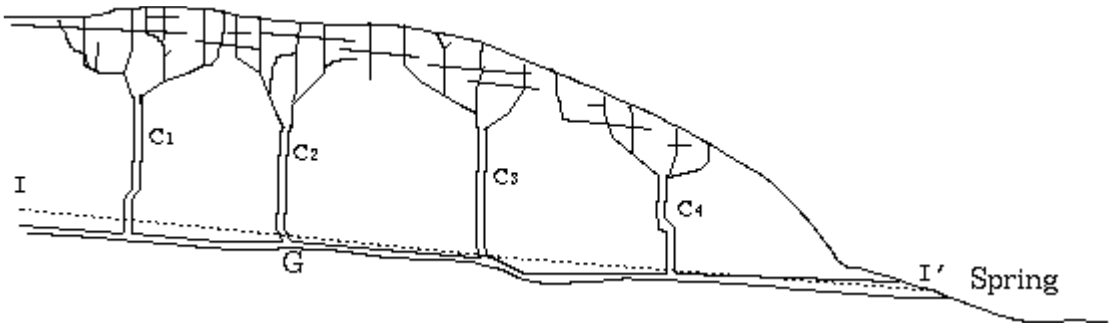

Figure 2: Diagram of karstic system: at the surface, fractures and infiltration joints; C1-C4, shafts with rapidly descending water; G horizontal gallery of karst flowage; I-I' water level (Cavaille, 1964).

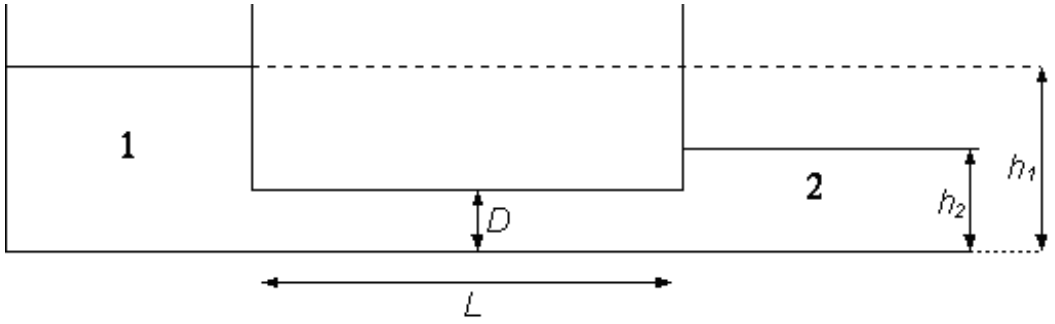

Figure 3: Schematic of water exchange between two reservoirs with hydraulic heads h_1, h_2 through a tunnel with length L and height D.

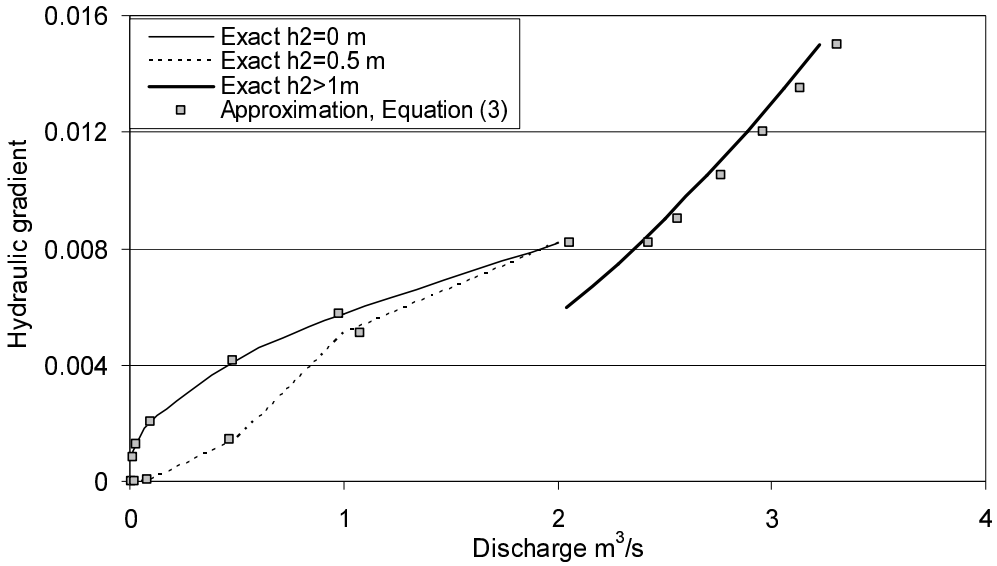

Figure 4: Hydraulic gradient-discharge curves and approximation with equation (3) for the tunnel of Figure 3 and for water level in reservoir 2 equal 0, 0.5 (open channel flow) and greater than 1 (pressurized flow).

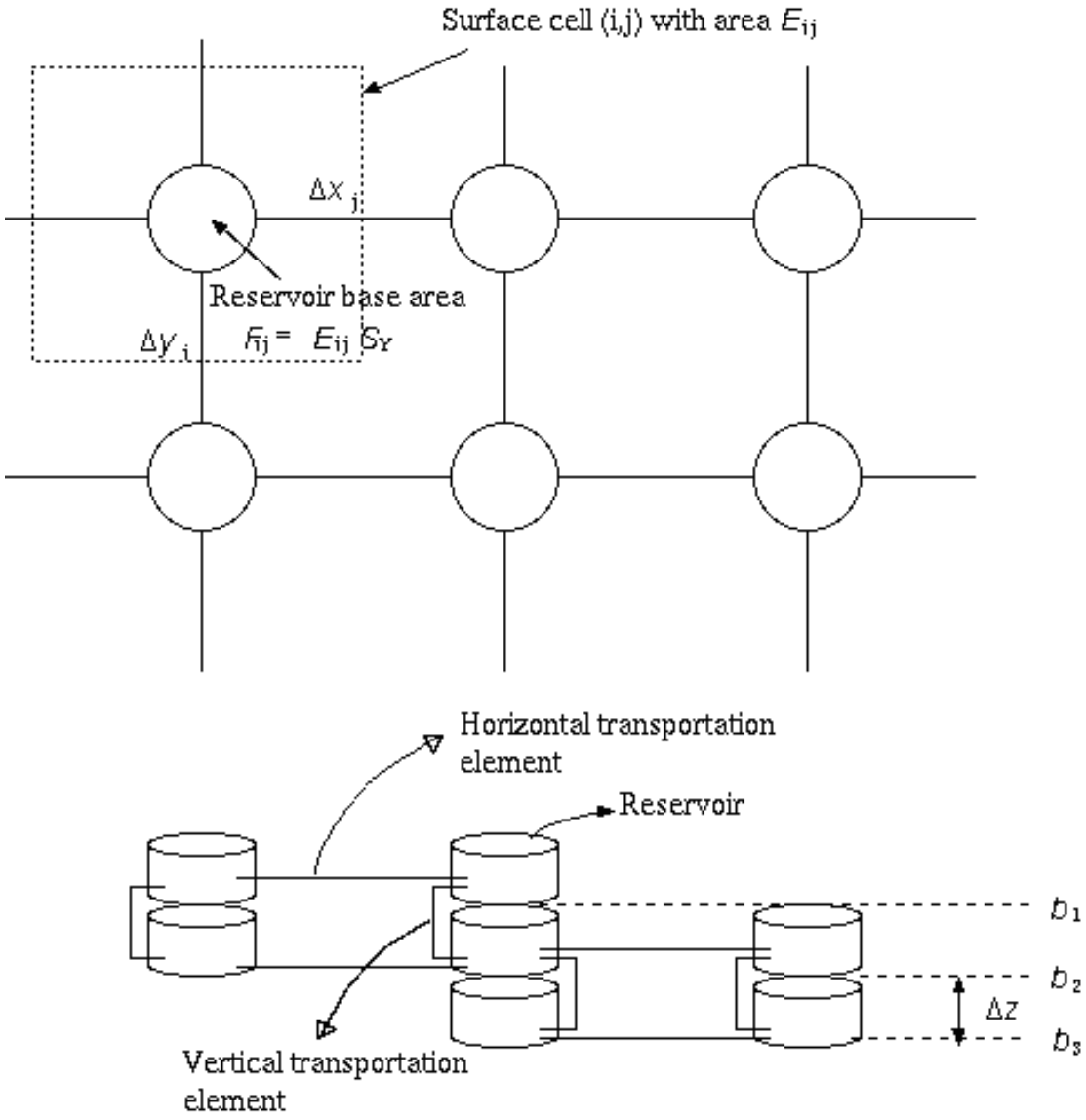

Figure 5: Horizontal view (upper panel) and vertical section (lower panel) of an aquifer with specific yield S_Y represented by a hydraulic analogue with three layers at heights b_1, b_2, b_3 (with equidistance Δz), consisting of transportation elements with lengths Δx_j or Δy_i and storage elements with base F_{ij} which corresponds to surface cell area E_{ij}.

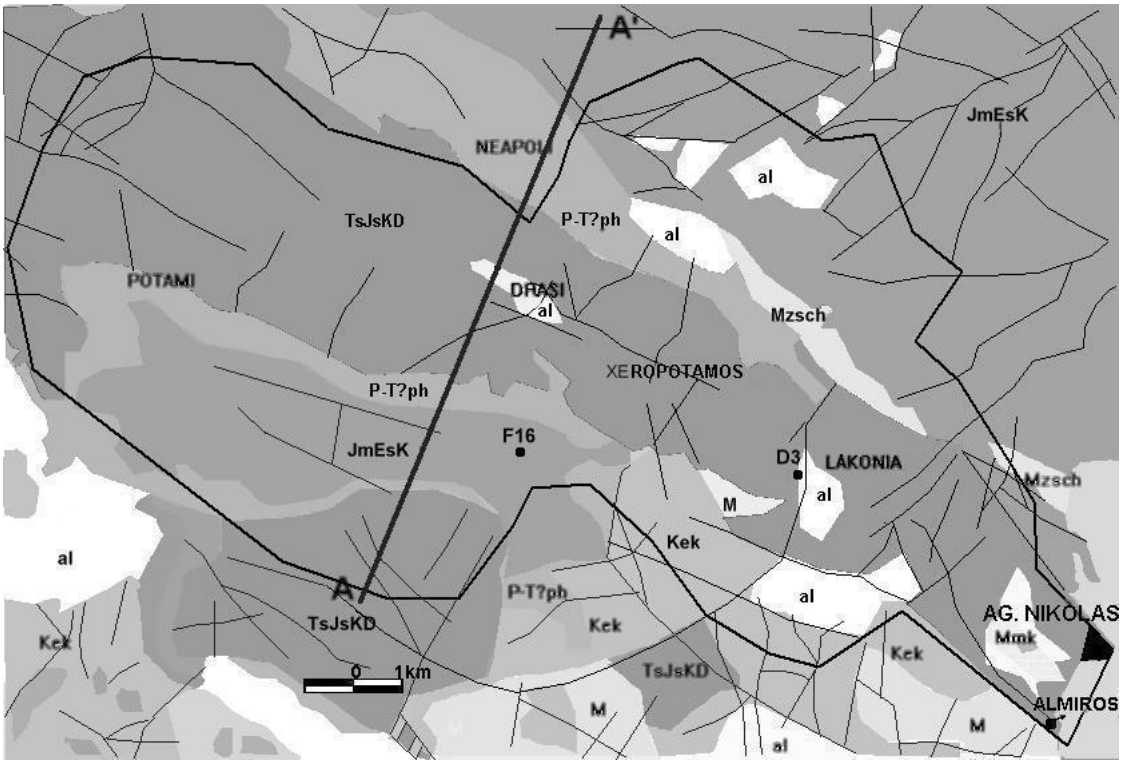

Figure 6: Catchment area and geology of the Almiros spring according to IGME 1977 (TsJsKD: dolomitic limestones, P-T?ph: phyllite-quartzite series, al: alluvium deposits, Kek: limestones, M: marly beds, Mzsch: carbonate-quartzose schists, Mmk: clastic rock formations, JmEsK: platy limestones). The Almiros spring is visible at the southeast corner of the map. The locations of the two observations wells F16 and D3 are marked on the map with dots.

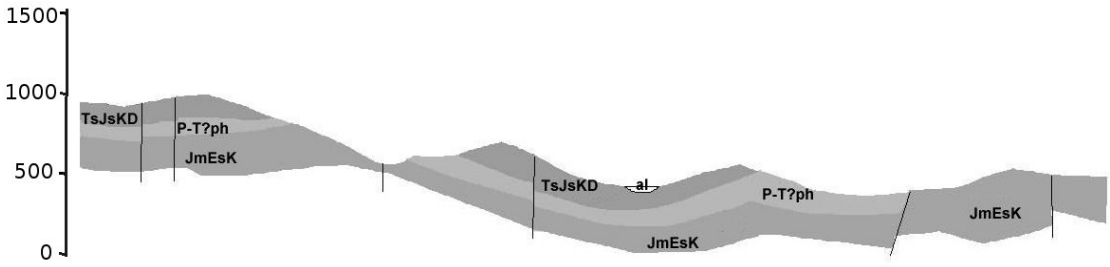

Figure 7: Cross section AA´ of Figure 6 (elevations in m; IGME, 1977).

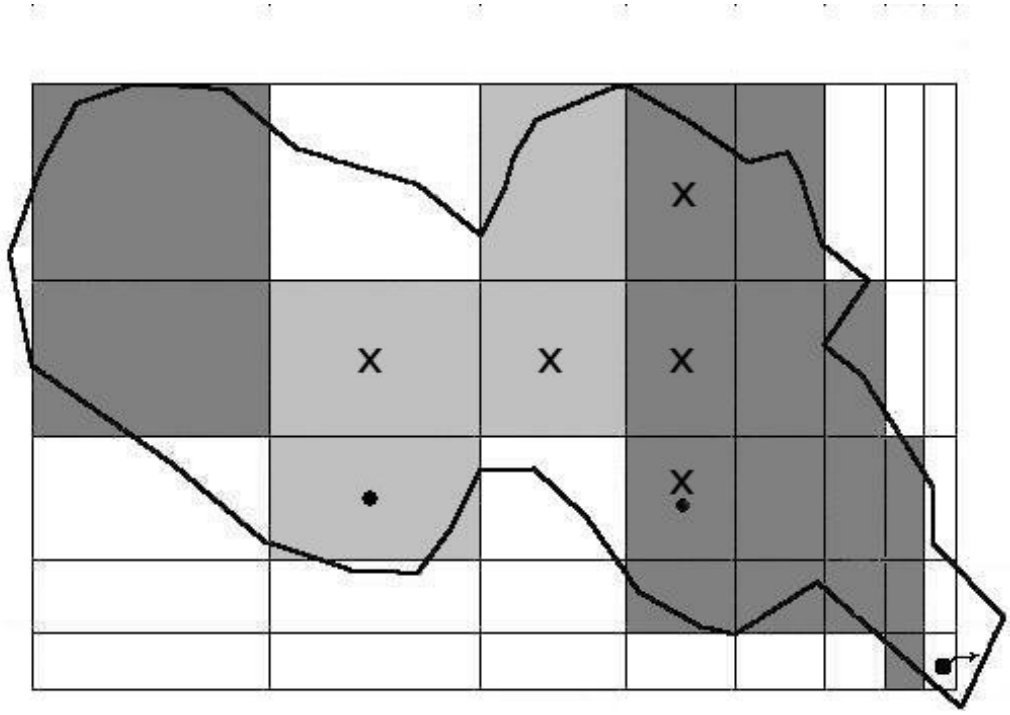

Figure 8: 5x8 discretisation of the Almiros spring aquifer where the dark and grey rectangles represent areas with generalised conductivity $c_{x,1}$ and $c_{x,2}$ respectively, and white rectangles represent no flow areas. The irrigated areas with pumped water are marked with x. The two cells closer to the observations wells are marked with dots (left F16, right D3).

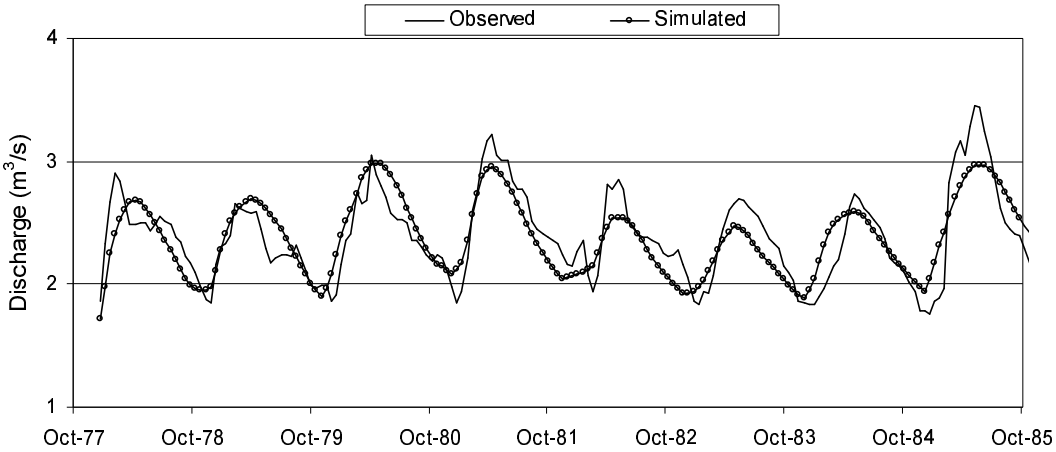

Figure 9: Observed and simulated discharge of the Almiros spring.

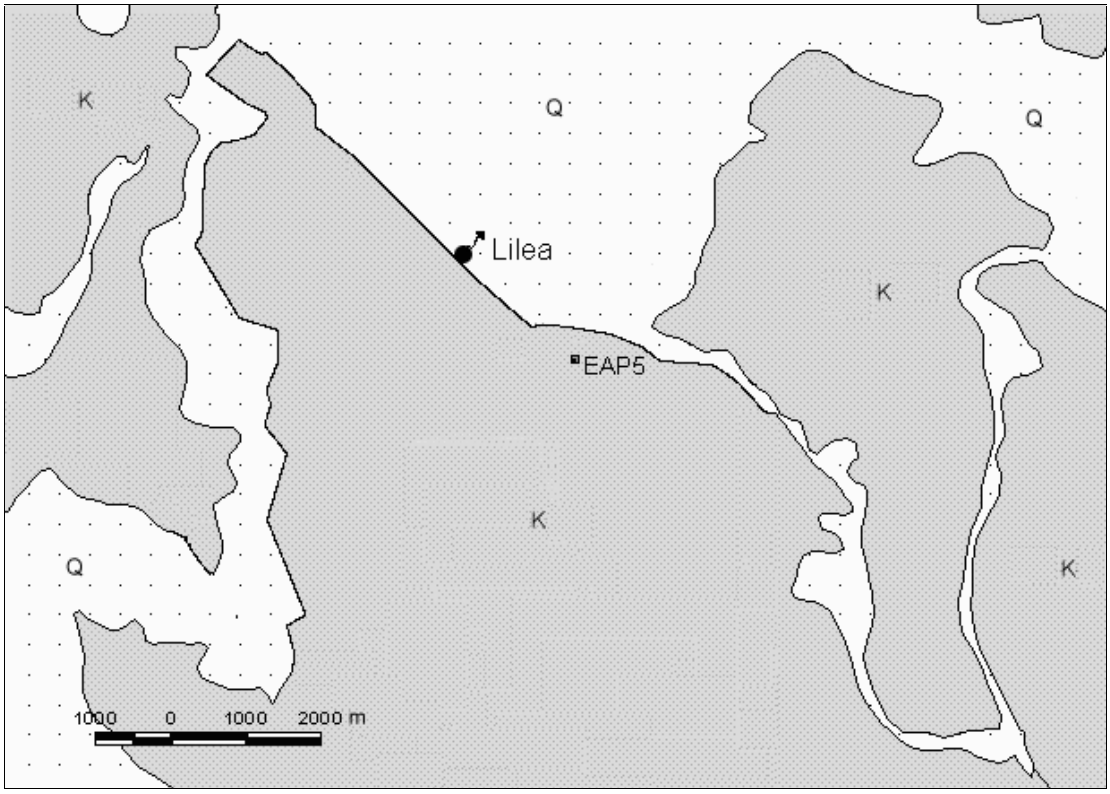

Figure 10: Geologic map of the Lilea spring aquifer according to IGME 1962 (Q alluvial deposits, K limestones) also indicating the location of the observation well EAP5.

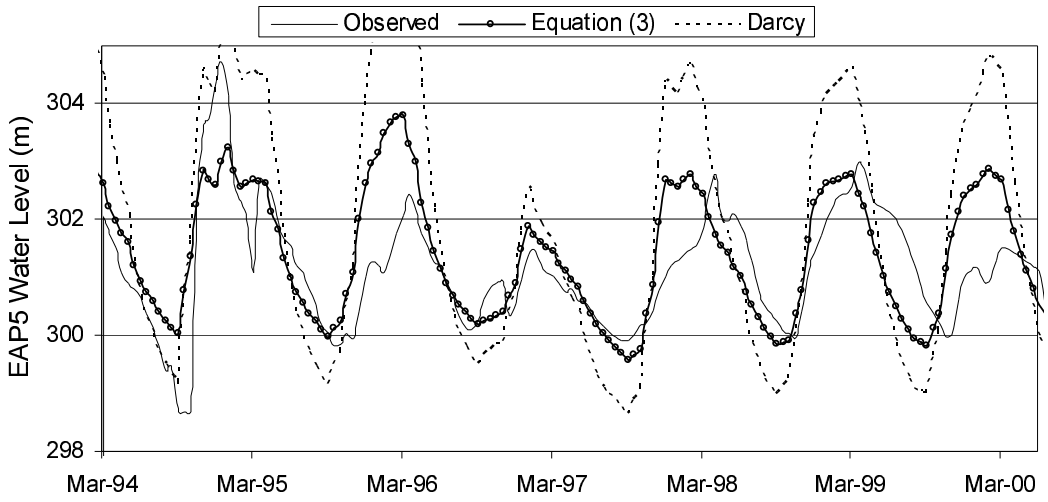

Figure 11: Observed and simulated water level at the EAP5 borehole in period 1994-2000 with parameters optimised for period 1981-1989.

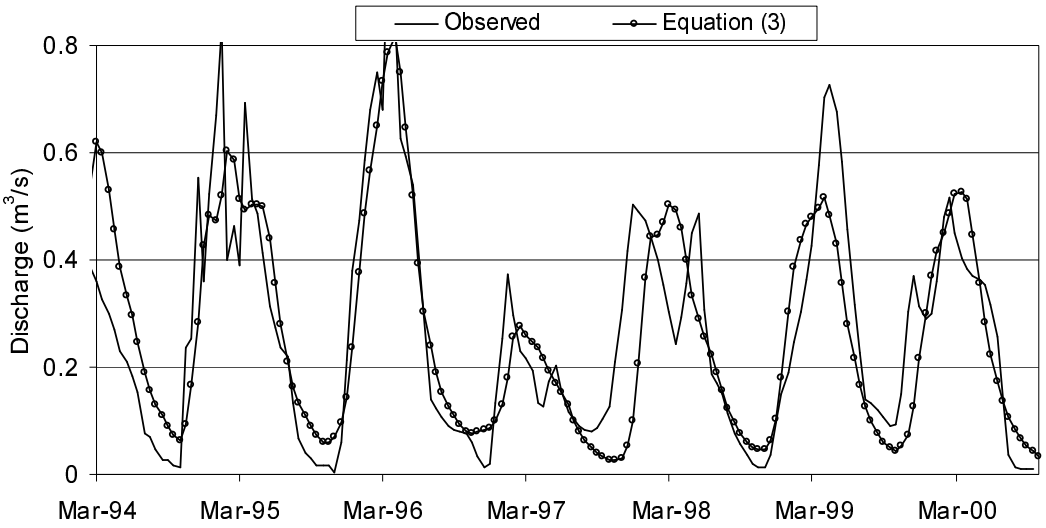

Figure 12: Observed and simulated spring hydrographs of the Lilea spring after optimisation in period 1994-2000.

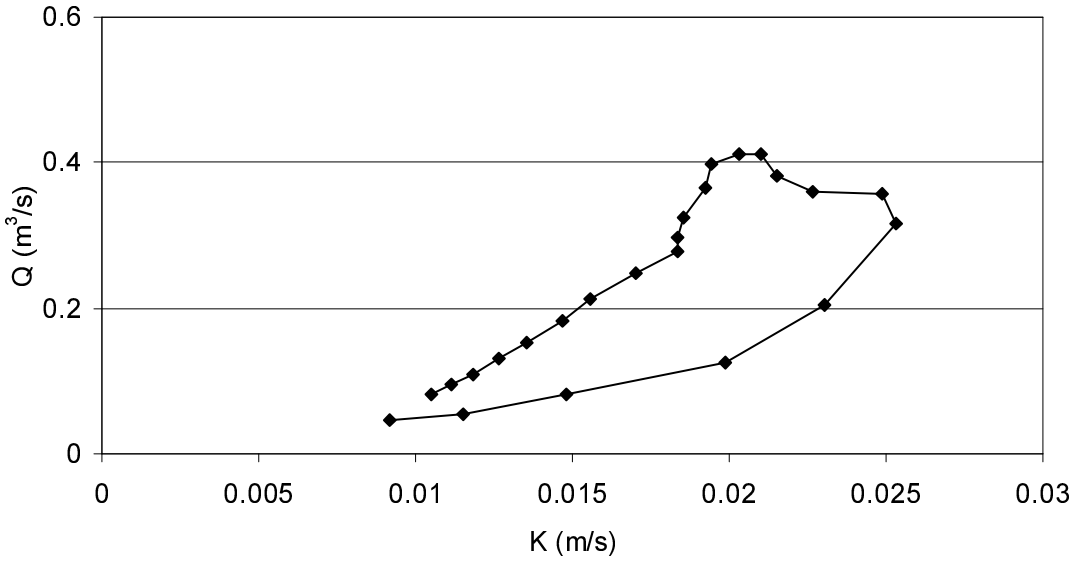

Figure 13: Estimated effective hydraulic conductivity using data from Lilea Aquifer model.

Appendix

1. MODFLOW and 3dkflow h-V equation

In this section we show that the h-V relations of MODFLOW and 3dkflow are equivalent. This is proved for the case where h_m, h_{m-1} < TOP and for the case where h_m < TOP, h_{m-1} > TOP. The proof for the rest cases is similar.

From the geometry of vertical discretisation we have:

$$\mathrm{TOP} = \Delta z + b \tag{a1}$$

From definitions of λ and F we have:

$$\lambda := \frac{S_Y}{S} \tag{a2}$$

$$F := \Delta x \, \Delta y \, S_Y \tag{a3}$$

In case of phreatic conditions we have h_m, h_{m-1} < TOP and W_m, W_{m-1} < dz. In this case equation (4) given that V = F W writes:

$$h_m = \frac{V_m}{F} + b \tag{a4}$$

$$h_{m-1} = \frac{V_{m-1}}{F} + b \tag{a5}$$

Substituting (a3) and subtracting (a5) from (a4) we obtain:

$$\Delta V = S_Y \, \Delta x \, \Delta y \, \Delta h \tag{a6}$$

which is the equation used in MODFLOW.

In the case where h_m < TOP, h_{m-1} > TOP it will be also W_m < Δz and W_{m-1} > Δz. In this case equation 4 writes for time m:

$$h_m = \frac{V_m}{F} + b \tag{a7}$$

or

$$V_m = (h_m - b) \, F \tag{a8}$$

and for time m-1:

$$h_{m-1} = (\frac{V_{m-1}}{F} - \Delta z)\,\lambda + b + \Delta z \qquad \text{(a9)}$$

or

$$V_{m-1} = [\,\frac{1}{\lambda}\,(h_{m-1} - b - \Delta z) + \Delta z\,]\,F \qquad \text{(a10)}$$

Subtracting (a10) from (a8) we obtain:

$$\Delta V = h_m\,F - b\,F - \frac{F}{\lambda}(\,h_{m-1} - b - \Delta z) - F\,\Delta z \qquad \text{(a11)}$$

Substituting (a1), (a2) and (a3) to (a11) we obtain:

$$\Delta V = [S_Y\,(h_m - TOP) + S\,(TOP - h_{m-1})\,]\,\Delta x\,\Delta y \qquad \text{(a12)}$$

which is the equation used in MODFLOW.